Dynamics of the viral community on the cheese surface during maturation and persistence across production years

Thomas Paillet, Quentin Lamy-Besnier, Clarisse Figueroa, Marie-Agnès Petit, Eric Dugat-Bony

Dynamics of the viral community on the cheese surface during maturation and persistence across production years

Thomas Paillet,[a] Quentin Lamy-Besnier,[b] Clarisse Figueroa,[a]* Marie-Agnès Petit,[b] Eric Dugat-Bony[a]#

[a]Université Paris-Saclay, INRAE, AgroParisTech, UMR SayFood, 91120 Palaiseau, France

[b]Université Paris-Saclay, INRAE, AgroParisTech, Micalis Institute, 78352 Jouy-en-Josas, France

Running Head: Viral dynamics and persistence on the cheese surface

#Address correspondence to Eric Dugat-Bony, eric.dugat-bony@inrae.fr.

*Present address: Université de Paris Cité, INSERM, IAME, UMR 1137, 75018 Paris, France

ABSTRACT

The surface of smear-ripened cheeses constitutes a dynamic microbial ecosystem resulting from the successive development of different microbial groups. Recent studies indicate that a viral community, mainly composed of bacteriophages, coexists with cellular microorganisms in this ecosystem, but its ecological significance remains to be elucidated. In this work, we studied a French smear-ripened cheese by both viral metagenomics and 16S metabarcoding approaches to assess both the dynamics of phages and bacterial communities on the cheese surface during the ripening period, and their persistence in ready-to-eat cheeses over the years of production. We observed a clear transition of the phage community structure during ripening with a decreased relative abundance of viral species (vOTUs) associated with *Lactococcus* phages, which were replaced by vOTUs associated with phages infecting ripening bacteria such as *Brevibacterium, Glutamicibacter, Pseudoalteromonas* and *Vibrio*. The dynamics of the phage community was strongly associated with bacterial successions observed on the cheese surface. Finally, a core of abundant vOTUs were systematically detected in ready-to-eat cheeses produced at different dates spanning more than 4 years of production, indicating long-term persistence of the main phages in the cheese production environment. Together, these findings offer novel perspectives on the ecology of bacteriophages in smear-ripened cheese and emphasize the significance of incorporating bacteriophages in the microbial ecology studies of fermented foods.

IMPORTANCE

Smear-ripened cheeses are microbial ecosystems made up of various microorganisms including bacteria, yeasts and also viruses such as bacteriophages, which infect and regulate bacterial populations. In this work, a French smear-ripened cheese was used to study how these viruses and bacteria interact over time and during cheese production. It revealed that the composition of the bacteriophage community shifts during the ripening process, aligning with the bacterial successions observed on the cheese surface between lactic acid bacteria and ripening bacteria. Additionally, the vast majority of these bacteriophages were found consistently in cheese products made over a 4-years period, showing that they represent a persistent component of the cheese-making environment. This research highlights the importance of considering these bacteriophages when studying the microbial life of fermented foods like cheese.

INTRODUCTION

Due to their unique ripening process, involving frequent washes with saline and/or alcoholic solutions, smear-ripened cheeses host a peculiar and diverse microbiota composed of lactic acid bacteria (LAB, mainly starter cultures added at the beginning of the process for milk acidification), yeasts and salt-tolerant bacteria belonging to the Actinomycetota, Bacillota and Pseudomonadota phyla (1). The surface microbiota of smear-ripened cheeses is considered to be responsible for the typical flavour and organoleptic properties of this type of cheese (2). From the past two decades, numerous studies have been conducted to describe the composition of this microbiota using isolation-based methods (3, 4), molecular fingerprinting (5–8), and more recently amplicon-based metagenomics also commonly referred to as metabarcoding (9–12).

Time series studies also enabled to reveal microbial successions occurring on the surface of smear-ripened cheeses during the maturation process (8, 13). Lactic acid bacteria (LAB), usually originating from starter cultures, grow first in the milk and represent the dominant microorganisms in the curd. Yeasts, *e.g. Debaryomyces hansenii* and *Geotrichum candidum*, which exhibit acid tolerance and metabolize lactate, subsequently colonize the cheese surface, resulting in its deacidification. With the pH increase, the establishment of a diverse bacterial community is progressively observed. The most common bacterial taxa detected at the end of ripening on smear-ripened cheese belong to coryneform bacteria (*e.g.* species of the *Glutamicibacter*, *Brevibacterium*, *Corynebacterium* or *Brachybacterium* genera), *Staphylococcus* species and halophilic or halotolerant gram-negative bacteria (*e.g.* species of the *Psychrobacter*, *Halomonas*, *Pseudoalteromonas, Hafnia, Vibrio*, *Pseudomonas* or *Proteus* genera) (14).

Microbial interactions are key biotic factors determining the structure and functioning of cheese microbial ecosystems and, ultimately, affecting cheese quality and safety (15, 16). In many natural ecosystems, bacteriophage infections shapes the composition of bacterial populations (17) and recent work suggests the same applies to fermented foods (18, 19). In the dairy industry, the impact of LAB phages is well documented because their lytic activity can disturb the milk acidification step, causing

delay in the production and even total loss of production (20, 21). Consequently, the most studied dairy phages are *Lactococcus*, *Streptococcus*, *Lactobacillus* and *Leuconostoc* phages, infecting the main starter cultures (22). Viral metagenomics has been recently employed to characterize the bacteriophage communities in dairy samples, including whey (23) and cheeses (24, 25). These investigations have demonstrated that such viral communities are not restricted to LAB phages, but encompass a diverse array of phages that could potentially also infect non-inoculated and ripening bacteria during cheese production.

However, only few studies report the isolation of such virulent phages from cheese infecting ripening bacteria, *i.e.* *Propionibacterium freudeunreichii* and *Brevibacterium aurantiacum* (26–28). We also isolated in a previous work five new virulent phages, targeting *Glutamicibacter arilaitensis*, *Brevibacterium aurantiacum*, *Psychrobacter aquimaris* and *Leuconostoc falkenbergense*, from the surface of a French smear-ripened cheese suggesting that predation is likely to occur on such ecosystems for most of the dominant bacteria (29). However, little is known about their ecology. In this study, our aim was to enhance our understanding of the temporal distribution of bacteriophages and their bacterial hosts on the surface of a French smear-ripened cheese across two distinct time scales. Initially, cheeses were obtained directly from the production facility at five distinct ripening stages over 28 days, to analyze phage dynamics throughout a production cycle (Figure 1, dynamic study). Subsequently, ready-to-eat cheeses of the same brand and variety were sampled in 2017, 2019, and 2022 to assess the long-term persistence of phages in this ecosystem (persistence study).

RESULTS

Composition of the cheese surface virome.

The sequence assembly obtained from all the studied samples (15 from the dynamic study and 9 from the persistence study) led to the production of a metavirome composed of 331 vOTUs >2 Kb (Table 1). The vast majority of these contigs (284) were detected in samples from both the dynamic and persistence studies.

The most abundant phages detected in the dataset were identified as *Lactococcus* phages from the 949 and 936 groups (*Audreyjarvisvirus* and *Skunavirus* genera, respectively) and *Glutamicibacter* phage

Montesquieu (Table 2). Of importance, the five virulent phages previously isolated from the same cheese, namely Montesquieu, Voltaire, Rousseau, D'Alembert and Diderot were also detected in this metagenomics survey. Remarkably, the vOTUs with no match (BLAT identity × coverage < 30%) to any known dairy phages (Table S1) represented only 3% of the relative abundance in the dataset, showing that most of the dominant phages present in this ecosystem have already close-relatives that have been isolated and characterized.

The composition of the viral community present on the cheese surface evolves through the ripening process.

The effect of each production step on the cheese virome composition was assessed by computing Bray-Curtis dissimilarity (BC). The PERMANOVA test indicated a significant effect of this variable (p-value = 0.001, R^2=0.658) and the principal coordinate analysis revealed that the first axis clearly discriminates samples from the first 3 washes (NaCl) and samples from the two last washes (NaCl + alcoholic liquor) (Figure 2A). The second axis helps discriminating samples from the third wash (W3) and samples from the two first (W1 and 2). Regarding the viral diversity, as estimated by the Shannon index, a slight decrease was noted from W3 onwards. However, this decrease was not statistically significant, suggesting that there were no major alterations of the viral diversity related to the production step ($p>0.05$, Kruskal-Wallis test; Figure 2B).

In order to visualize the abundance of the different vOTUs in the samples, we kept only those with a normalized relative abundance above $5x10^{-5}$ in average (168 contigs) and represented their distribution across samples through a heatmap (Figure 2C). Three blocks of vOTUs were detected. The first one (top of the figure) was characterized by contigs whose abundance do not vary with the ripening and that corresponded mainly to virulent *Lactococcus* phages belonging to the 936 group (*Skunavirus* genus). The second block (bottom of the figure) contained contigs whose abundance decreased with ripening and that corresponded to other *Lactococcus* phages, close to the P335 group containing both temperate and virulent members (here qualified as ex-temperate phages). Finally, the third block (middle of the figure) was essentially composed of a few vOTUs that increased in relative abundance with ripening. These mainly corresponded to phages targeting ripening bacteria such as *Brevibacterium*, *Glutamicibacter*, *Pseudoalteromonas* and *Vibrio*, and non-starter lactic acid bacteria

(NSLAB) such as *Leuconostoc*. These few vOTUs correspond to uncharacterized phages, except *Glutamicibacter* phage Montesquieu, *Brevibacterium* phage Rousseau and *Leuconostoc* phage Diderot which we previously isolated from the same type of cheese.

As observed by the principal coordinate analysis of the Bray-Curtis dissimilarity (Figure 2A), the virome composition was similar between samples from W1 and W2, and between samples from W4 and W5 indicating the presence of two main viral communities, according to these two ripening stages. Samples from W3 exhibited a composition in between samples from W1-2 and W4-5 reflecting a transition stage captured in those samples.

Phage community shift during ripening follows changes in bacterial composition.

We then applied the DESeq2 method to identify differentially abundant viral contigs between the two stable stages represented by W1-2 and W4-5 samples (Figure 3A). Interestingly, two groups emerged, with very readable outlines: vOTUs corresponding to phages infecting starter cultures, such as *Lactococcus* and *Streptococcus* phages, had a negative log2 fold change meaning their relative abundances significantly decreased during the ripening process. Conversely, vOTUs of virulent phages targeting NSLAB and ripening bacteria (e.g. *Brevibacterium*, *Glutamicibacter*, *Pseudoalteromonas* and *Vibrio*) were significantly more abundant in W4-5 samples compared to W1-2 samples (positive log2 fold change) reflecting a higher population level for such phages on the cheese surface in later ripening stages. Among them were two vOTUs with high similarity to the genomes of *Glutamicibacter* phage Montesquieu (2017-3_NODE2; 47,703 bp; 100% identity × coverage by BLAT), and *Brevibacterium* phage Rousseau (2022-5_NODE4; 41,077 bp; 54% identity × coverage by BLAT but 98% identity at the nucleotidic level over a portion of >9 kb). In this group, we also detected a vOTU partially related to *Brevibacterium* phage AGM1 (SA2-0_NODE10; 37148 bp; 3.5% identity × coverage by BLAT but 88% identity at the nucleotidic level over a portion of 1324 nt), which was isolated from a Canadian washed-rind cheese.

The composition of the bacterial community of the cheese surface also varied through the ripening process (Figure 3B). As for the virome composition, we observed a clear transition in the bacterial community structure from W3 onwards. *Lactococcus* was the dominant genus in samples from W1 and W2, and was progressively replaced by typical surface aerobic bacteria such as members of

Psychrobacter, *Vibrio*, *Glutamicibacter* and *Pseudoalteromonas* genera. Based on plate counts (Figure 3 C-E), this results should be mainly attributed to the growth of aerobic bacteria (~ 2 logs increase between W1 and W5, from ~ 10^8 to ~ 10^{10} CFU/g) since lactic acid remained stable over time (~ 10^8 CFU/g) during the whole kinetic. This shift indicates that changes observed on the phage community structure is strongly associated with bacterial successions on the cheese surface.

The dominant fraction of the cheese virome persists across production years.

The effect of the production year (2017, 2019 and 2022) on the composition of the virome of the cheese surface (ready-to-eat cheeses, meaning after packaging and storage) was assessed by computing Bray-Curtis dissimilarity (Figure 4A). The PERMANOVA test indicated a significant effect of this factor (p-value of 0.002, R2 = 0.814) suggesting structural variations of the phage community across production years. The principal coordinate analysis revealed that the first axis clearly discriminates 2019 samples from 2017 and 2022 samples. The second axis helps discriminating samples from years 2017 and 2022.

The heatmap visualization showed that the vast majority of the most abundant contigs were shared among the 3 production years and that only a few low-abundant contigs were detected specifically in one or two production years (blue zones on the graph) (Figure 4C). This result is congruent with the stability of the bacterial community composition over the three sampling campaigns (Figure 4B).

We then evaluated the proportion of vOTUs that were shared across production year. When using the complete dataset (no filtering on relative abundance, Figure 4D), we observed that 56.6% of the 297 vOTUs present in at least one of the three years were shared in all production years (75.4% in two different production years). Interestingly, samples from year 2022 had a higher number of unique vOTUs (48, 32.1% of the total) than samples from years 2017 and 2019 (3 and 11, respectively). We next applied the same analysis only on the most abundant vOTUs (average normalized relative abundance > 5×10^{-5}, 99 vOTUs in total) (Figure 4E). The vast majority of the vOTUs, *i.e.* 89.9%, were shared among the 3 productions years and this value rose to 97% when considering only two different years. This result indicates that the cheese surface virome was mostly stable in terms of composition (presence/absence) and that dominant phages persist across productions years. The disparity between production years, as detected by beta-diversity analysis, may therefore primarily be

attributed to the presence or absence of phages in low abundance, and fluctuations in the relative abundance of dominant phages.

DISCUSSION

Recent studies of cheese samples using viral metagenomics (24, 25) or exploration of cheese microbial metagenomes (30) have revealed that the cheese environment harbours a diverse bacteriophage community whose targets go beyond lactic acid starter cultures. The isolation of a few representatives of these non-starter phages (27–29) suggests that phage activity occurs in this ecosystem, raising the question of their overall impact on microbial successions during the ripening process. Recently, the deliberate addition of one of those phages, *Brevibacterium* phage AGM9, was proven to slow down the development of the orange rind color in a model system mimicking a smear-ripened cheese (31). In the present study, we described the viral community of a French smear ripened cheese over time, by combining two timescales: the 28-days long ripening process, as well as from ready-to-eat cheeses spanning four years of production. The virome was predominantly composed of vOTUs associated with a variety of *Lactococcus* phages as well as the *Glutamicibacter* phage Montesquieu, a virulent phage we had previously isolated from the same cheese variety (29). This phage targets the ripening bacterium *Glutamicibacter arilaitensis*. Several other phages were detected at sub-dominant levels. Among them, only a few, such as the *Brevibacterium* phage Rousseau, *Leuconostoc* phage Diderot, *Psychrobacter* phage d'Alembert, *Glutamicibacter* phage Voltaire, and a novel vOTU displaying minimal sequence homology to *Brevibacterium* phage AGM1, have been previously documented in cheese. The diversity of these sub-dominant phages is therefore not yet completely sampled and, in particular, underscores the necessity to isolate a more comprehensive collection of phages from this ecosystem. Notably, we identified vOTUs that partially aligned with genomic sequences from phages infecting halotolerant bacteria (e.g., *Pseudoalteromonas*, *Halomonas*, *Vibrio*, and *Proteus* species). Even though these bacteria are not intentionally inoculated into smear-ripened cheese, they tend to dominate by the end of the ripening process (14). Their phages should therefore be looked for in future isolation initiatives.

The dynamics of bacterial and fungal communities has been extensively studied in a wide diversity of cheese products during ripening (13, 32–36), enabling to accurately describe cellular successions occurring in cheese production processes (16). In this study, we present the first analysis of viral dynamics throughout cheese ripening. Similar to the observed transitions in bacteria and fungi, there was a distinct shift in viral composition over the course of the ripening process. Some vOTUs associated with LAB starter-phages, primarily targeting *Lactococcus lactis*, were progressively replaced by vOTUs specific to phages that infect ripening bacteria. When comparing phage to bacterial dynamics, there was a notable relationship between phage trajectories and bacterial successions on the cheese surface. Specifically, the relative abundance of phages exhibited a concomitant increase with the relative abundance of their predicted bacterial hosts. This findings is of importance since the increase in the relative abundance of a specific vOTU within a virome can be interpreted as indicative of the active replication of the corresponding phage and further suggests the presence of a predator-prey interaction within the investigated ecosystem.

Surprisingly, despite the changes in bacterial and viral communities' composition during the production process, the relative abundance of some vOTUs remained very stable during ripening. They mainly corresponded to virulent *Lactococcus* phages, belonging to the *Skunavirus* genus (formerly 936 group). Among *Lactococcus* phages, this genus is by far the most frequently detected in the dairy industry (37). Given that *Lactococcus lactis* predominantly proliferates during milk acidification and maintains consistent concentration levels throughout the ripening period in this type of cheese (13), we theorize that the maintenance of *Skunavirus* is indicative of the stability of phage particles produced at the onset of cheese maturation. The remarkable stability of *Skunavirus* particles in comparison to other *Lactococcus* phage groups, especially the P335 group, has been reported earlier (38, 39). In contrast, we suggest that the relative decline observed in our experiment for certain *Lactococcus* phages, specifically those affiliated to the P335 group, denotes their temporal instability. Nevertheless, a more comprehensive examination of this phenomenon warrants dedicated investigations.

Cheese microbial communities of washed-rind cheese are generally dominated by environmental microorganisms detected in processing environments, the so-called "house" microbiota (40), which is specific to each production facility and provides a microbial signature distinguishing cheeses belonging to the same variety but manufactured by distinct producers (10). Recently, the analysis of several Quebec's terroir cheeses revealed that the dominant microorganisms remain stable from year to year, which could be linked to typical manufacturing practices and consistency in the use of starter and ripening cultures by cheesemakers (41). Here, we describe a similar observation for bacteriophages. We indeed identified a core-virome composed of a large proportion of the most abundant vOTUs, consistently detected across four production years. Previous work on an undefined starter culture used for the production of a Swiss-type cheese, propagated for decades in the same dairy environment, revealed that phages and bacteria stably coexist over time in this system and suggests that this may contribute to the stable maintenance of the cheese starter culture over years (42). The same may apply for phages and bacteria on the surface of smear-ripened cheese since both are contaminating the cheese production environment, and are therefore likely to repeatedly contaminate cheese from one production cycle to another (29, 40).

In conclusion, the observed dynamics of the cheese virome throughout the ripening process, coupled with its relative persistence across production years, support an important role of bacteriophages in the cheese microbial ecosystem. Recognizing this biotic factor is essential for a comprehensive understanding of microbial successions during milk fermentation. Moreover, this knowledge may offer cheesemakers novel avenues to refine and control their production processes.

MATERIAL AND METHODS

Cheese samples.

(i) Dynamic study design: French smear-ripened cheeses, all from the same production batch, were collected directly from the cheese plant at five different stages during the ripening process (Figure 1). These stages, labeled W1 to W5, correspond to distinct washing steps. The initial three washes utilized a NaCl solution, while the final two employed a NaCl solution supplemented with increasing

concentrations of alcoholic liquor. At each stage, three distinct cheeses were sampled and designated as replicates A, B, and C. Cheeses were immediately stored at 4°C after sampling and processed within 48h.

(ii) Persistence study design: ready-to-consume cheeses of the same type and same brand as the previously described cheeses were purchased in a local supermarket in December 2017, November 2019 and February 2022, spanning >4 years of production. Three different cheeses, with the same production date, were sampled each year and used as replicates. Cheeses were immediately stored at 4°C after sampling and processed within 48h.

For both dynamic and persistence studies, cheese samples were analysed immediately after reception at the lab. Using sterile knives, the rind, approximately 2-3 mm thick, was carefully separated from the core. It was then blended and processed for microbial counts, viral DNA extraction for metavirome analysis, and microbial DNA extraction for extensive amplicon sequencing targeting the 16S rRNA gene, which will be subsequently referred to as 16S metabarcoding.

Microbiological analysis.

Bacteria and yeasts were enumerated by plating serial dilutions (10^{-1} to 10^{-7}) of one gram of cheese rind mixed in 9 mL of physiological water (9 g/L NaCl) on three different culture media. Brain Heart Infusion Agar (BHI, Biokar Diagnostics) supplemented with 50 mg/L amphotericin (Sigma Aldrich, Saint-Louis, MO, USA) was used to count total aerobic bacteria after 48 h of incubation at 28°C. Man, Rogosa and Sharpe Agar (MRS, Biokar Diagnostics, Allonne, France) supplemented with 50 mg/L amphotericin was used to count lactic acid bacteria after 48 h of incubation at 30°C under anaerobic conditions. Yeasts were counted on Yeast Extract Glucose Chloramphenicol (YEGC, Biokar Diagnostics, Allonne, France) after 48 h of incubation at 28°C.

Viral DNA extraction and metavirome analysis.

Extraction of the viral fraction from cheese rind was performed according to protocol P4 detailed in (24) comprising a filtration step and a chloroform treatment. DNA was extracted from the viral particles according to the protocol described in the same study and sent to Eurofins Genomics for high throughput sequencing using the Illumina NovaSeq platform (2 × 150 bp paired-end reads, approximately 10 million reads per sample).

All the details about the tools, versions and parameters used in the following pipeline are available in scripts deposited in the GitLab repository (https://forgemia.inra.fr/eric.dugat-bony/cheese_virome). Briefly, raw reads were quality filtered using Trimmomatic v0.39 (43). Then a single assembly was computed for the collection of triplicate reads from each sample with Spades v3.15.3 (44), using either the complete dataset of trimmed reads available or after subsampling the dataset to 1.5 million, 150,000 or 15,000 trimmed reads per sample. We noted that some abundant contigs were assembled into longer, nearly complete contigs, after subsampling. Contigs of length >2kb from all assemblies were selected and clustered following an approach adapted from (45). Succinctly, a pairwise alignment was first performed for all contigs using BLAT (46). Then, contigs with a self-alignment > 110% of contig length, corresponding to chimeras, were removed. Remaining contigs were clustered at the species level (90% identity × coverage) and the longest contig within each cluster was selected as the representative sequence. The final contig dataset consisted in 3122 dereplicated contigs.

Viral contigs were selected using a combination of three detection tools: VIBRANT v1.2.1 (47), VirSorter2 v2.2.4 (48) and CheckV v0.8.1 (49). The ones retained in the final virome were those meeting at least one of the following criteria: declared “complete”, “high” or “medium” quality by either VIBRANT or CheckV, declared “full” by VirSorter2. The bacterial host of the 332 viral contigs was predicted using iPHoP (50). Finally, all sequences were compared by BLAT to an in-house database consisting of genome sequences from 32 common dairy phages (listed in Table S1) in order to identify potential related phages with known taxonomy, verified host and lifestyle (30% identity × coverage minimal cutoff). When appropriate, the host genus predicted by iPHoP was replaced by the genus of the bacterial host of the closest relative phage identified by the BLAT search. One contig, corresponding to the genome of the phage PhiX174 which is routinely used as control in Illumina sequencing runs to monitor sequencing quality, was discarded resulting in a final dataset of 331 viral contigs.

In order to evaluate the relative abundance of each viral contig in each metavirome sample, trimmed reads were mapped against the viral contigs using bwa-mem2 v2.2.1 (51) and counted with Msamtools v1.0.0 profile with the options --multi=equal --unit=ab –nolen (https://github.com/arumugamlab/msamtools). The output files from all samples were joined into an

abundance table and processed using the R package phyloseq v1.38.0 (52). For each experimental dataset (dynamic study, persistence study), read counts were rarefied to the minimum depth observed in one individual sample. Then, read counts were normalized by contig length and transformed to relative abundances, in order to enable both comparison of the viral community structure between samples and comparison of the abundance level between contigs. Making the assumption that one viral contig corresponds to one species (which is wrong each time several contigs belonging to the same phage genome are present), Bray-Curtis dissimilatory index, as computed by the distance function from the R package phyloseq, was used to compare viral communities between samples and the effect of different variables on their structure was assessed using permutational analysis of variance as computed by the adonis2 function from the R package vegan v2.6-2.

For the dynamic dataset, differential analysis was performed on raw counts using the DESeq function implemented in the DESeq2 package v1.38.0 (53). Indeed, this function already includes a normalization step (by the median of ratios method). Contigs were considered differentially abundant if adjusted pvalue > 0.01, log2 fold change > 3 or < -3 and average raw counts > 1500.

Microbial DNA extraction and 16S metabarcoding profiles.

Total DNA extraction from the cheese surface was performed as previously described (10). PCR amplification of the V3-V4 regions of the 16S rRNA gene was performed with the primers V3F (5'-ACGGRAGGCWGCAG-3') and V4R (5'-TACCAGGGTATCTAATCCT-3') carrying the Illumina 5'-CTTTCCCTACACGACGCTCTTCCGATCT-3' and the 5'-GGAGTTCAGACGTGTGCTCTTCCGATCT-3' tails, respectively. The reaction was performed using 10 ng of extracted DNA, 0.5 µM primer, 0.2 mM dNTP, and 2.5 U of the MTP Taq DNA polymerase (Sigma-Aldrich, USA). The amplification was carried out using the following program: 94°C for 60 s, 30 cycles at 94°C for 60 s, 65°C for 60 s, 72°C for 60 s, and a final elongation step at 72°C for 10 min. The resulting PCR products were sent to the @BRIDGe platform (INRAE, Jouy-en-Josas, France) for library preparation and sequencing. Briefly, amplicons were purified using a magnetic beads CleanPCR (Clean NA, GC biotech B.V., The Nederlands), the concentration was measured using a Nanodrop spectrophotometer (Thermo Scientific, USA) and the amplicon quality was assessed on a Fragment Analyzer (AATI, USA) with the reagent kit ADNdb 910 (35-1,500 bp).

Sample multiplexing was performed by adding tailor-made 6 bp unique indexes during the second PCR step which was performed on 50–200 ng of purified amplicons using the following program: 94°C for 10 min, 12 cycles at 94°C for 60 s, 65°C for 60 s, 72°C for 60 s, and a final elongation step at 72°C for 10 min. After purification and quantification (as described above), all libraries were pooled with equal amounts in order to generate equivalent number of raw reads for each library. The DNA concentration of the pool was quantified on a Qubit Fluorometer (Thermofisher Scientific, USA) and adjusted to a final concentration between 5 and 20 nM for sequencing. The pool was denatured (NaOH 0.1N) and diluted to 7 pM. The PhiX Control v3 (Illumina, USA) was added to the pool at 15% of the final concentration, as described in the Illumina procedure, and the mixture was loaded onto the Illumina MiSeq cartridge according to the manufacturer's instructions using MiSeq Reagent Kit v3 (2 × 250 bp paired-end reads).

Paired-end reads were analysed using FROGS v3.2 (54), according to the standard operating procedure. Briefly, operational taxonomic units (OTUs) were built using Swarm with an aggregation distance of 1 and the --fastidious option (55), and each OTU that accounted for <0.005% of the total dataset of sequences was discarded, as previously recommended (56). Lastly, the OTU's affiliation was checked using the EzBiocloud database v52018 (57). The abundance table was processed using the R package phyloseq v1.38.0 (52).

Data availability.

Raw sequencing data for cheese virome and bacterial microbiome were deposited at the sequence read archive (SRA) of the NCBI (https://www.ncbi.nlm.nih.gov/sra/) as part of bioprojects PRJNA984302 (dynamic study) and PRJNA984735 (persistence study).

ACKNOWLEDGMENTS

T.P. is the recipient of a doctoral fellowship from the French Ministry of Higher Education, Research and Innovation (MESRI) and the MICA department of the French National Research Institute for Agriculture, Food and Environment (INRAE). For the metabarcoding analysis, this work has benefited from the facilities and expertise of @BRIDGe (Université Paris-Saclay, INRAE, AgroParisTech, GABI, 78350 Jouy-en-Josas, France). We are also grateful to the INRAE MIGALE bioinformatics

facility (MIGALE, INRAE, 2020. Migale bioinformatics Facility, doi: 10.15454/1.5572390655343293E12) for providing computing and storage resources.

TABLES

Table 1: summary statistics about the metavirome dataset.

	Complete dataset (24 samples)	Dynamic study (15 samples)	Persistence study (9 samples)
Total number of vOTUs > 2 Kb	331	318	297
Number of vOTUs with relative abundance > 5×10^{-5}	157	168	99

Table 2: Most abundant dairy phages detected on the cheese metavirome. Phages that have been previously isolated from the same cheese variety are highlighted in bold. When classification is available at the International Committee on Taxonomy of Viruses (ICTV), the viral genus is denoted in brackets.

Closest relatives	Relative abundance*
Lactococcus 949 group *(Audreyjarvisvirus)*	0.56
***Glutamicibacter* Montesquieu**	**0.23**
Lactococcus 936 group *(Skunavirus)*	0.18
Lactococcus P335 group	1.54E-03
***Brevibacterium* Rousseau**	**1.08E-03**
***Psychrobacter* D'Alembert**	**1.74E-04**
Leuconostoc* Diderot *(Limdunavirus)	**1.14E-04**
***Glutamicibacter* Voltaire**	**1.70E-05**
Streptococcus 987 group	7.87E-06

Lactococcus KSY1 group *(Chopinvirus)*	5.94E-07
Non dairy phages**	0.03

*The relative abundance value used here is not normalized by genome size, it corresponds to the relative proportion of reads mapping to all vOTUs belonging to a given phage group present in our in-house dairy phage database (Table S1).

**vOTUs without any match to our in-house dairy phage database (30% identity × coverage minimal cutoff).

FIGURE LEGENDS

Figure 1: Schematic representation of the experimental plan followed for the dynamic study of the virome composition during the ripening process. Samples were respectively obtained after each washing step (blue arrows indicate washes performed with a NaCl solution, red arrows indicate washes performed with a NaCl solution containing alcoholic liquor)**.**

Figure 2: Dynamic of the cheese surface virome along the ripening process. A) Principal coordinate analysis of the Bray-Curtis dissimilarity. Samples are coloured according the ripening step. B) Comparison of the viral diversity, estimated by the Shannon index, at the different ripening steps. C) Heatmap representing the normalized relative abundance of the most abundant vOTUs present in the dataset (168 vOTUs with an averaged normalized relative abundance value 5×10^{-5}) in the different samples. The colours on the heatmap represent the log-transformed relative abundance, and range from blue to red, blue indicating lower relative abundance and red indicating higher relative abundance. When available, vOTU annotations were indicated such as the host genus as predicted by iPHoP, the group of known phages it belongs to and its lifestyle.

Figure 3: Relationship between phage dynamic and the composition of cheese bacterial community. A) Differential abundance analysis on the virome data between the two stable stages represented by W1-2 and W4-5 samples. Log2 fold change values obtained for differential abundant

vOTUs (points) are represented and the dot colour indicate the predicted host genus according to iPHoP. Grey dots: no predicted host. B) Composition of the bacterial community assessed by a metabarcoding approach targeting the V3-V4 regions of the 16S rRNA gene. Three different cheeses from the same batch were analysed at each sampling point. Data were aggregated at the genus level. C) Yeasts counts expressed in log(CFU/g). D) Aerobic bacteria counts expressed in log(CFU/g). E) Lactic acid bacteria counts expressed in log(CFU/g).

Figure 4: Persistence of the cheese surface virome across production years. A) Principal coordinate analysis of the Bray-Curtis dissimilarity. Samples are coloured according the production year (2017, 2019 and 2022). B) Composition of the bacterial community assessed by a metabarcoding approach targeting the V3-V4 regions of the 16S rRNA gene. Three different cheeses from the same production year were analysed. Data were aggregated at the genus level. C) Heatmap representing the normalized relative abundance of the most abundant vOTUs (99 with an averaged normalized relative abundance value > 5×10^{-5}) in each sample. The colours on the heatmap represent the log-transformed relative abundance, and range from blue to red, blue indicating lower relative abundance and red indicating higher relative abundance. D) Venn diagram constructed from the dataset without filtering, comprising 297 vOTUs. E) Venn diagram constructed from the filtered dataset comprising 99 vOTUs with an averaged normalized relative abundance value > 5×10^{-5}.

SUPPLEMENTARY MATERIAL

Table S1. Common dairy phages and associated information.

REFERENCES

1. Mounier J, Coton M, Irlinger F, Landaud S, Bonnarme P. 2017. Chapter 38 - Smear-Ripened Cheeses, p. 955–996. *In* McSweeney, PLH, Fox, PF, Cotter, PD, Everett, DW (eds.), Cheese (Fourth Edition). Academic Press, San Diego.

2. Corsetti A, Rossi J, Gobbetti M. 2001. Interactions between yeasts and bacteria in the smear surface-ripened cheeses. International Journal of Food Microbiology 69:1–10.

3. Larpin-Laborde S, Imran M, Bonaïti C, Bora N, Gelsomino R, Goerges S, Irlinger F, Goodfellow M, Ward AC, Vancanneyt M, Swings J, Scherer S, Guéguen M, Desmasures N. 2011. Surface microbial consortia from Livarot, a French smear-ripened cheese. Canadian Journal of Microbiology 57:651–660.

4. Lavoie K, Touchette M, St-Gelais D, Labrie S. 2012. Characterization of the fungal microflora in raw milk and specialty cheeses of the province of Quebec. Dairy Sci & Technol 92:455–468.

5. Feurer C, Irlinger F, Spinnler H e., Glaser P, Vallaeys T. 2004. Assessment of the rind microbial diversity in a farmhouse-produced vs a pasteurized industrially produced soft red-smear cheese using both cultivation and rDNA-based methods. Journal of Applied Microbiology 97:546–556.

6. Mounier J, Monnet C, Jacques N, Antoinette A, Irlinger F. 2009. Assessment of the microbial diversity at the surface of Livarot cheese using culture-dependent and independent approaches. International Journal of Food Microbiology 133:31–37.

7. Mounier J, Gelsomino R, Goerges S, Vancanneyt M, Vandemeulebroecke K, Hoste B, Scherer S, Swings J, Fitzgerald GF, Cogan TM. 2005. Surface Microflora of Four Smear-Ripened Cheeses. Appl Environ Microbiol 71:6489–6500.

8. Rea MC, Görges S, Gelsomino R, Brennan NM, Mounier J, Vancanneyt M, Scherer S, Swings J, Cogan TM. 2007. Stability of the Biodiversity of the Surface Consortia of Gubbeen, a Red-Smear Cheese. Journal of Dairy Science 90:2200–2210.

9. Delcenserie V, Taminiau B, Delhalle L, Nezer C, Doyen P, Crevecoeur S, Roussey D, Korsak N, Daube G. 2014. Microbiota characterization of a Belgian protected designation of origin cheese, Herve cheese, using metagenomic analysis. Journal of Dairy Science 97:6046–6056.

10. Dugat-Bony E, Garnier L, Denonfoux J, Ferreira S, Sarthou A-S, Bonnarme P, Irlinger F. 2016. Highlighting the microbial diversity of 12 French cheese varieties. International Journal of Food Microbiology 238:265–273.

11. Quigley L, O'Sullivan O, Beresford TP, Ross RP, Fitzgerald GF, Cotter PD. 2012. High-throughput sequencing for detection of subpopulations of bacteria not previously associated with artisanal cheeses. Applied and Environmental Microbiology 78:5717–5723.

12. Wolfe BE, Button JE, Santarelli M, Dutton RJ. 2014. Cheese rind communities provide tractable systems for in situ and in vitro studies of microbial diversity. Cell 158:422–433.

13. Irlinger F, Monnet C. 2021. Temporal differences in microbial composition of Époisses cheese rinds during ripening and storage. Journal of Dairy Science 104:7500–7508.

14. Kothe CI, Bolotin A, Kraïem B-F, Dridi B, Renault P. 2021. Unraveling the world of halophilic and halotolerant bacteria in cheese by combining cultural, genomic and metagenomic approaches. International Journal of Food Microbiology 358:109312.

15. Irlinger F, Mounier J. 2009. Microbial interactions in cheese: implications for cheese quality and safety. Current Opinion in Biotechnology 20:142–148.

16. Mayo B, Rodríguez J, Vázquez L, Flórez AB. 2021. Microbial Interactions within the Cheese Ecosystem and Their Application to Improve Quality and Safety. 3. Foods 10:602.

17. Brown TL, Charity OJ, Adriaenssens EM. 2022. Ecological and functional roles of bacteriophages in contrasting environments: marine, terrestrial and human gut. Current Opinion in Microbiology 70:102229.

18. Ledormand P, Desmasures N, Dalmasso M. 2020. Phage community involvement in fermented beverages: an open door to technological advances? Critical Reviews in Food Science and Nutrition 1–10.

19. Paillet T, Dugat-Bony E. 2021. Bacteriophage ecology of fermented foods: anything new under the sun? Current Opinion in Food Science 40:102–111.

20. Garneau JE, Moineau S. 2011. Bacteriophages of lactic acid bacteria and their impact on milk fermentations. Microb Cell Fact 10 Suppl 1:S20.

21. Pujato S a., Quiberoni A, Mercanti D j. 2019. Bacteriophages on dairy foods. Journal of Applied Microbiology 126:14–30.

22. Marcó MB, Moineau S, Quiberoni A. 2012. Bacteriophages and dairy fermentations. Bacteriophage 2:149–158.

23. Muhammed MK, Kot W, Neve H, Mahony J, Castro-Mejía JL, Krych L, Hansen LH, Nielsen DS, Sørensen SJ, Heller KJ, Sinderen D van, Vogensen FK. 2017. Metagenomic analysis of dairy bacteriophages: extraction method and pilot study on whey samples derived from using undefined and defined mesophilic starter cultures. Appl Environ Microbiol 83:e00888-17.

24. Dugat-Bony E, Lossouarn J, De Paepe M, Sarthou A-S, Fedala Y, Petit M-A, Chaillou S. 2020. Viral metagenomic analysis of the cheese surface: A comparative study of rapid procedures for extracting viral particles. Food Microbiology 85:103278.

25. Queiroz LL, Lacorte GA, Isidorio WR, Landgraf M, de Melo Franco BDG, Pinto UM, Hoffmann C. 2022. High Level of Interaction between Phages and Bacteria in an Artisanal Raw Milk Cheese Microbial Community. mSystems 0:e00564-22.

498 26. Cheng L, Marinelli LJ, Grosset N, Fitz-Gibbon ST, Bowman CA, Dang BQ, Russell DA, Jacobs-Sera
499 D, Shi B, Pellegrini M, Miller JF, Gautier M, Hatfull GF, Modlin RL. 2018. Complete genomic
500 sequences of Propionibacterium freudenreichii phages from Swiss cheese reveal greater
501 diversity than Cutibacterium (formerly Propionibacterium) acnes phages. BMC Microbiology
502 18:19.

503 27. de Melo AG, Rousseau GM, Tremblay DM, Labrie SJ, Moineau S. 2020. DNA tandem repeats
504 contribute to the genetic diversity of Brevibacterium aurantiacum phages. Environmental
505 Microbiology 22:3413–3428.

506 28. Gautier M, Rouault A, Sommer P, Briandet R. 1995. Occurrence of Propionibacterium
507 freudenreichii bacteriophages in swiss cheese. Appl Environ Microbiol 61:2572–2576.

508 29. Paillet T, Lossouarn J, Figueroa C, Midoux C, Rué O, Petit M-A, Dugat-Bony E. 2022. Virulent
509 Phages Isolated from a Smear-Ripened Cheese Are Also Detected in Reservoirs of the Cheese
510 Factory. 8. Viruses 14:1620.

511 30. Walsh AM, Macori G, Kilcawley KN, Cotter PD. 2020. Meta-analysis of cheese microbiomes
512 highlights contributions to multiple aspects of quality. Nat Food 1:500–510.

513 31. de Melo AG, Lemay M-L, Moineau S. 2023. The impact of Brevibacterium aurantiacum virulent
514 phages on the production of smear surface-ripened cheeses. International Journal of Food
515 Microbiology 400:110252.

516 32. De Pasquale I, Di Cagno R, Buchin S, De Angelis M, Gobbetti M. 2014. Microbial Ecology
517 Dynamics Reveal a Succession in the Core Microbiota Involved in the Ripening of Pasta Filata
518 Caciocavallo Pugliese Cheese. Applied and Environmental Microbiology 80:6243–6255.

519 33. Flórez AB, Mayo B. 2006. Microbial diversity and succession during the manufacture and
520 ripening of traditional, Spanish, blue-veined Cabrales cheese, as determined by PCR-DGGE.
521 International Journal of Food Microbiology 110:165–171.

522 34. Fuka MM, Wallisch S, Engel M, Welzl G, Havranek J, Schloter M. 2013. Dynamics of Bacterial
523 Communities during the Ripening Process of Different Croatian Cheese Types Derived from Raw
524 Ewe's Milk Cheeses. PLoS ONE 8:e80734.

525 35. Larpin S, Mondoloni C, Goerges S, Vernoux J-P, Guéguen M, Desmasures N. 2006. *Geotrichum*
526 *candidum* dominates in yeast population dynamics in Livarot, a French red-smear cheese. FEMS
527 Yeast Research 6:1243–1253.

528 36. Pangallo D, Šaková N, Koreňová J, Puškárová A, Kraková L, Valík L, Kuchta T. 2014. Microbial
529 diversity and dynamics during the production of May bryndza cheese. International Journal of
530 Food Microbiology 170:38–43.

531 37. Jolicoeur AP, Lemay M-L, Beaubien E, Bélanger J, Bergeron C, Bourque-Leblanc F, Doré L,
532 Dupuis M-È, Fleury A, Garneau JE, Labrie SJ, Labrie S, Lacasse G, Lamontagne-Drolet M, Lessard-
533 Hurtubise R, Martel B, Menasria R, Morin-Pelchat R, Pageau G, Samson JE, Rousseau GM,
534 Tremblay DM, Duquenne M, Lamoureux M, Moineau S. 2023. Longitudinal Study of Lactococcus
535 Phages in a Canadian Cheese Factory. Applied and Environmental Microbiology 0:e00421-23.

536 38. Madera C, Monjardín C, Suárez JE. 2004. Milk contamination and resistance to processing
537 conditions determine the fate of Lactococcus lactis bacteriophages in dairies. Applied and
538 Environmental Microbiology 70:7365–7371.

539 39. Wagner N, Brinks E, Samtlebe M, Hinrichs J, Atamer Z, Kot W, Franz CMAP, Neve H, Heller KJ.
540 2017. Whey powders are a rich source and excellent storage matrix for dairy bacteriophages.
541 International Journal of Food Microbiology 241:308–317.

542 40. Bokulich NA, Mills DA. 2013. Facility-Specific “House” Microbiome Drives Microbial Landscapes
543 of Artisan Cheesemaking Plants. Applied and Environmental Microbiology 79:5214–5223.

544 41. Raymond-Fleury A, Lessard M-H, Chamberland J, Pouliot Y, Dugat-Bony E, Turgeon SL, St-Gelais
545 D, Labrie S. 2022. Analysis of Microbiota Persistence in Quebec’s Terroir Cheese Using a
546 Metabarcoding Approach. 7. Microorganisms 10:1381.

547 42. Somerville V, Berthoud H, Schmidt RS, Bachmann H-P, Meng YH, Fuchsmann P, von Ah U, Engel
548 P. 2021. Functional strain redundancy and persistent phage infection in Swiss hard cheese
549 starter cultures. ISME J 1–12.

550 43. Bolger AM, Lohse M, Usadel B. 2014. Trimmomatic: a flexible trimmer for Illumina sequence
551 data. Bioinformatics 30:2114–2120.

552 44. Bankevich A, Nurk S, Antipov D, Gurevich AA, Dvorkin M, Kulikov AS, Lesin VM, Nikolenko SI,
553 Pham S, Prjibelski AD, Pyshkin AV, Sirotkin AV, Vyahhi N, Tesler G, Alekseyev MA, Pevzner PA.
554 2012. SPAdes: a new genome assembly algorithm and its applications to single-cell sequencing.
555 J Comput Biol 19:455–477.

556 45. Shah SA, Deng L, Thorsen J, Pedersen AG, Dion MB, Castro-Mejía JL, Silins R, Romme FO,
557 Sausset R, Jessen LE, Ndela EO, Hjelmsø M, Rasmussen MA, Redgwell TA, Leal Rodríguez C,
558 Vestergaard G, Zhang Y, Chawes B, Bønnelykke K, Sørensen SJ, Bisgaard H, Enault F, Stokholm J,
559 Moineau S, Petit M-A, Nielsen DS. 2023. Expanding known viral diversity in the healthy infant
560 gut. 5. Nat Microbiol 8:986–998.

561 46. Kent WJ. 2002. BLAT—The BLAST-Like Alignment Tool. Genome Res 12:656–664.

562 47. Kieft K, Zhou Z, Anantharaman K. 2020. VIBRANT: automated recovery, annotation and curation
563 of microbial viruses, and evaluation of viral community function from genomic sequences.
564 Microbiome 8:90.

565 48. Guo J, Bolduc B, Zayed AA, Varsani A, Dominguez-Huerta G, Delmont TO, Pratama AA, Gazitúa
566 MC, Vik D, Sullivan MB, Roux S. 2021. VirSorter2: a multi-classifier, expert-guided approach to
567 detect diverse DNA and RNA viruses. Microbiome 9:37.

568 49. Nayfach S, Camargo AP, Schulz F, Eloe-Fadrosh E, Roux S, Kyrpides NC. 2021. CheckV assesses
569 the quality and completeness of metagenome-assembled viral genomes. 5. Nat Biotechnol
570 39:578–585.

571 50. Roux S, Camargo AP, Coutinho FH, Dabdoub SM, Dutilh BE, Nayfach S, Tritt A. 2022. iPHoP: an
572 integrated machine-learning framework to maximize host prediction for metagenome-
573 assembled virus genomes. preprint. Microbiology.

574 51. Vasimuddin Md, Misra S, Li H, Aluru S. 2019. Efficient Architecture-Aware Acceleration of BWA-
575 MEM for Multicore Systems, p. 314–324. *In* 2019 IEEE International Parallel and Distributed
576 Processing Symposium (IPDPS).

577 52. McMurdie PJ, Holmes S. 2013. phyloseq: an R package for reproducible interactive analysis and
578 graphics of microbiome census data. PLOS ONE 8:e61217.

579 53. Love MI, Huber W, Anders S. 2014. Moderated estimation of fold change and dispersion for
580 RNA-seq data with DESeq2. Genome Biology 15:550.

581 54. Escudié F, Auer L, Bernard M, Mariadassou M, Cauquil L, Vidal K, Maman S, Hernandez-Raquet
582 G, Combes S, Pascal G. 2017. FROGS: Find, Rapidly, OTUs with Galaxy Solution. Bioinformatics
583 https://doi.org/10.1093/bioinformatics/btx791.

584 55. Mahé F, Rognes T, Quince C, de Vargas C, Dunthorn M. 2014. Swarm: robust and fast clustering
585 method for amplicon-based studies. PeerJ 2:e593.

586 56. Bokulich NA, Subramanian S, Faith JJ, Gevers D, Gordon JI, Knight R, Mills DA, Caporaso JG.
587 2013. Quality-filtering vastly improves diversity estimates from Illumina amplicon sequencing.
588 Nat Methods 10:57–59.

589 57. Yoon S-H, Ha S-M, Kwon S, Lim J, Kim Y, Seo H, Chun J. 2017. Introducing EzBioCloud: a
590 taxonomically united database of 16S rRNA gene sequences and whole-genome assemblies. Int
591 J Syst Evol Microbiol 67:1613–1617.

592

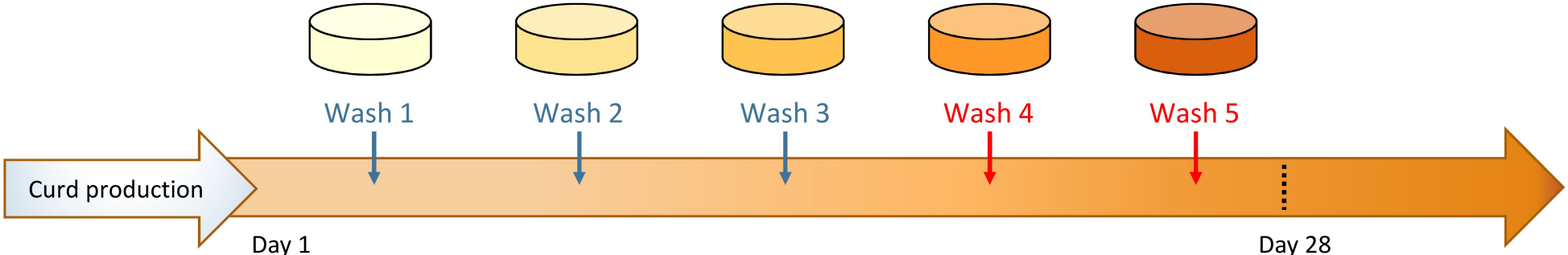
Wash 1
Wash 2
Wash 3
Wash 4
Wash 5
Curd production
Day 1
Day 28

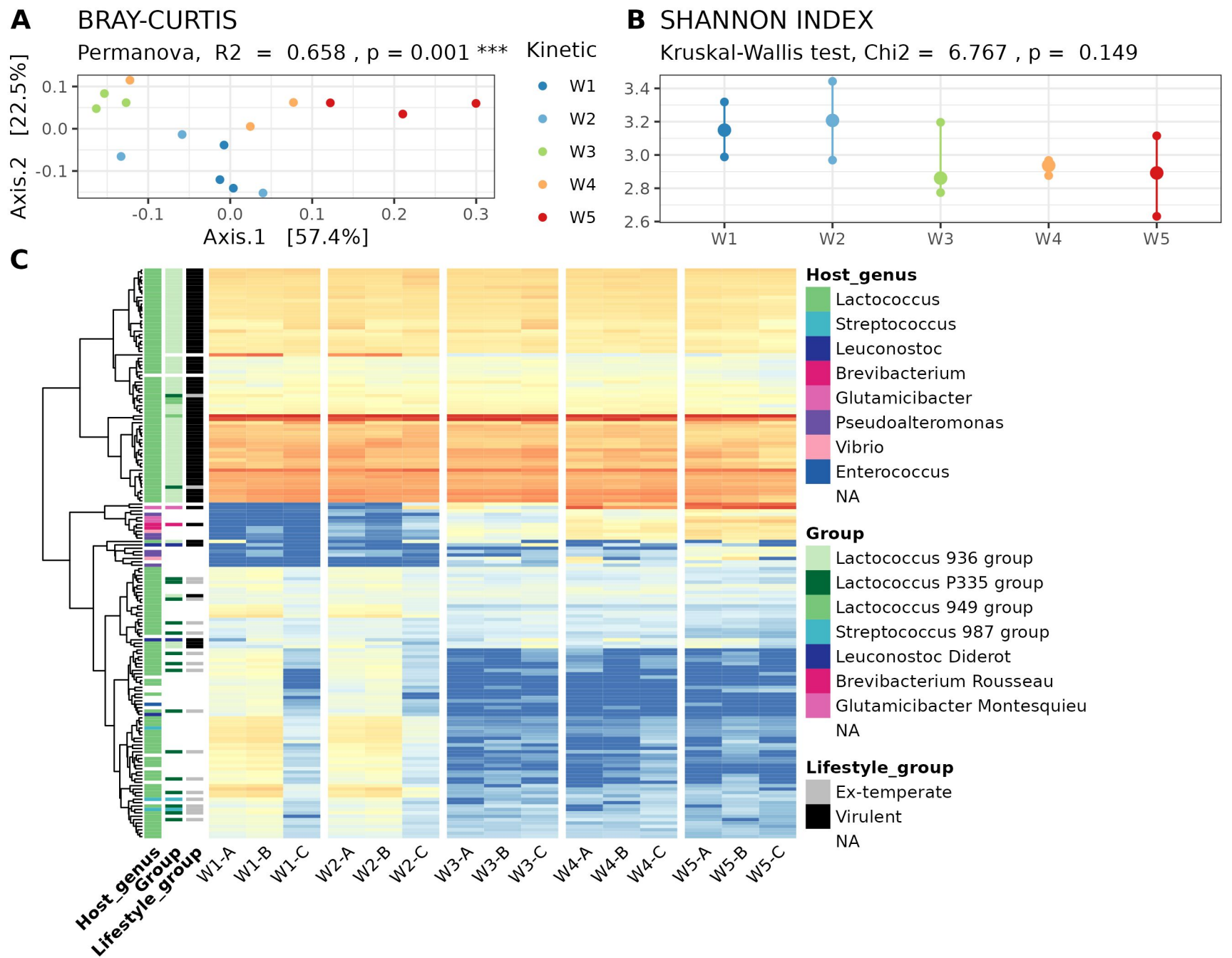
A
BRAY-CURTIS
Permanova, R2 = 0.658 , p = 0.001 ***
Kinetic
W1
W2
W3
W4
W5
Axis.2 [22.5%]
Axis.1 [57.4%]
B
SHANNON INDEX
Kruskal-Wallis test, Chi2 = 6.767 , p = 0.149
C
Host_genus
Lactococcus
Streptococcus
Leuconostoc
Brevibacterium
Glutamicibacter
Pseudoalteromonas
Vibrio
Enterococcus
NA
Group
Lactococcus 936 group
Lactococcus P335 group
Lactococcus 949 group
Streptococcus 987 group
Leuconostoc Diderot
Brevibacterium Rousseau
Glutamicibacter Montesquieu
NA
Lifestyle_group
Ex-temperate
Virulent
NA
Host_genus
Group
Lifestyle_group
W1-A
W1-B
W1-C
W2-A
W2-B
W2-C
W3-A
W3-B
W3-C
W4-A
W4-B
W4-C
W5-A
W5-B
W5-C

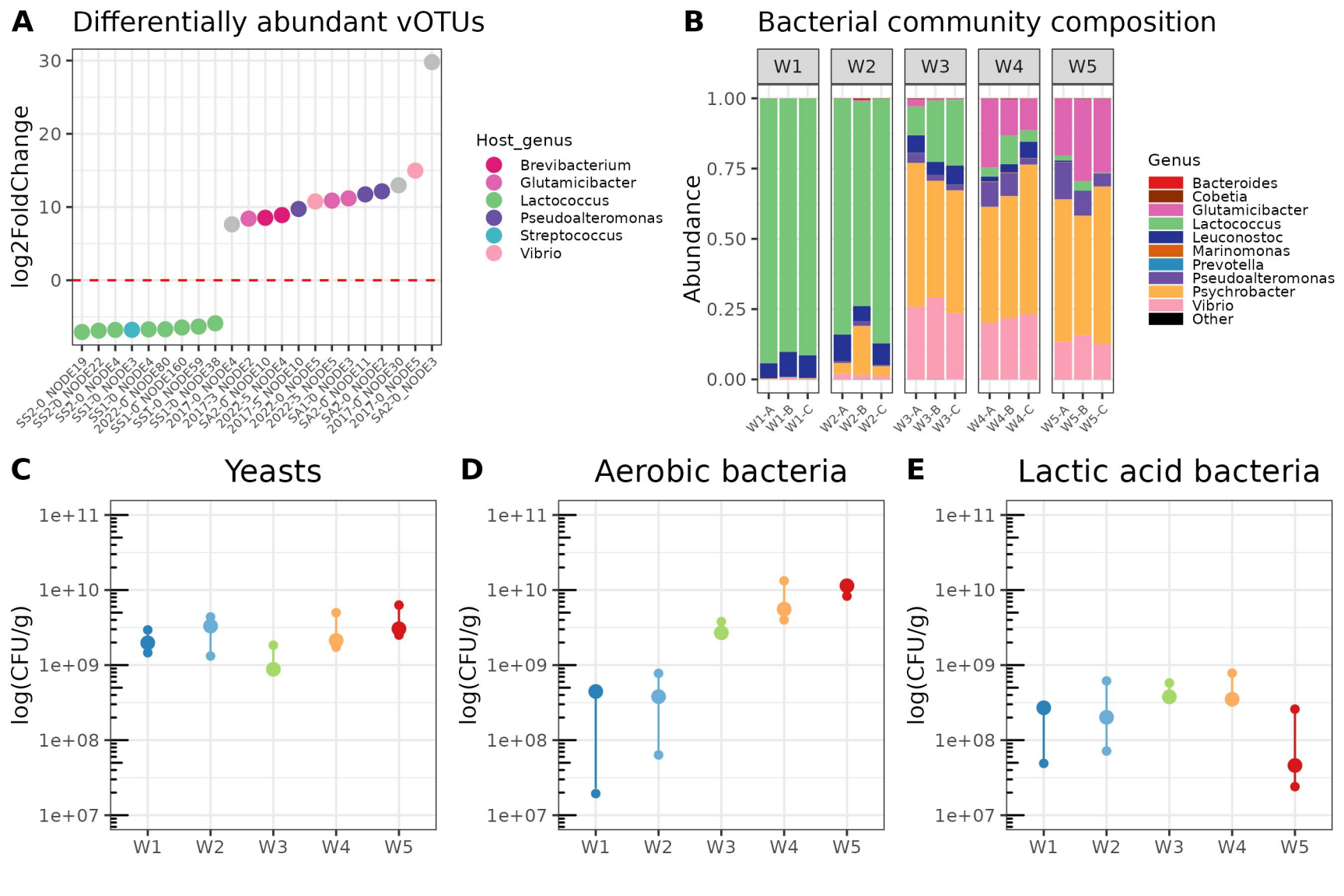
A
Differentially abundant vOTUs
log2FoldChange
30
20
10
0
SS2-0_NODE19
SS2-0_NODE22
SS2-0_NODE4
SS1-0_NODE3
SS1-0_NODE4
2022-0_NODE80
SS1-0_NODE160
SS1-0_NODE59
SS1-0_NODE38
2017-0_NODE4
201773_NODE2
SA2-0_NODE10
2022-5_NODE4
2017-5_NODE10
2022-0_NODE5
2022-5_NODE5
SA1-0_NODE3
SA2-0_NODE11
SA2-0_NODE2
2017-0_NODE30
2017-0_NODE5
SA2-0_NODE3
Host_genus
Brevibacterium
Glutamicibacter
Lactococcus
Pseudoalteromonas
Streptococcus
Vibrio
B
Bacterial community composition
W1
W2
W3
W4
W5
Abundance
1.00
0.75
0.50
0.25
0.00
W1-A
W1-B
W1-C
W2-A
W2-B
W2-C
W3-A
W3-B
W3-C
W4-A
W4-B
W4-C
W5-A
W5-B
W5-C
Genus
Bacteroides
Cobetia
Glutamicibacter
Lactococcus
Leuconostoc
Marinomonas
Prevotella
Pseudoalteromonas
Psychrobacter
Vibrio
Other
C
Yeasts
log(CFU/g)
1e+11
1e+10
1e+09
1e+08
1e+07
W1
W2
W3
W4
W5
D
Aerobic bacteria
log(CFU/g)
1e+11
1e+10
1e+09
1e+08
1e+07
W1
W2
W3
W4
W5
E
Lactic acid bacteria
log(CFU/g)
1e+11
1e+10
1e+09
1e+08
1e+07
W1
W2
W3
W4
W5

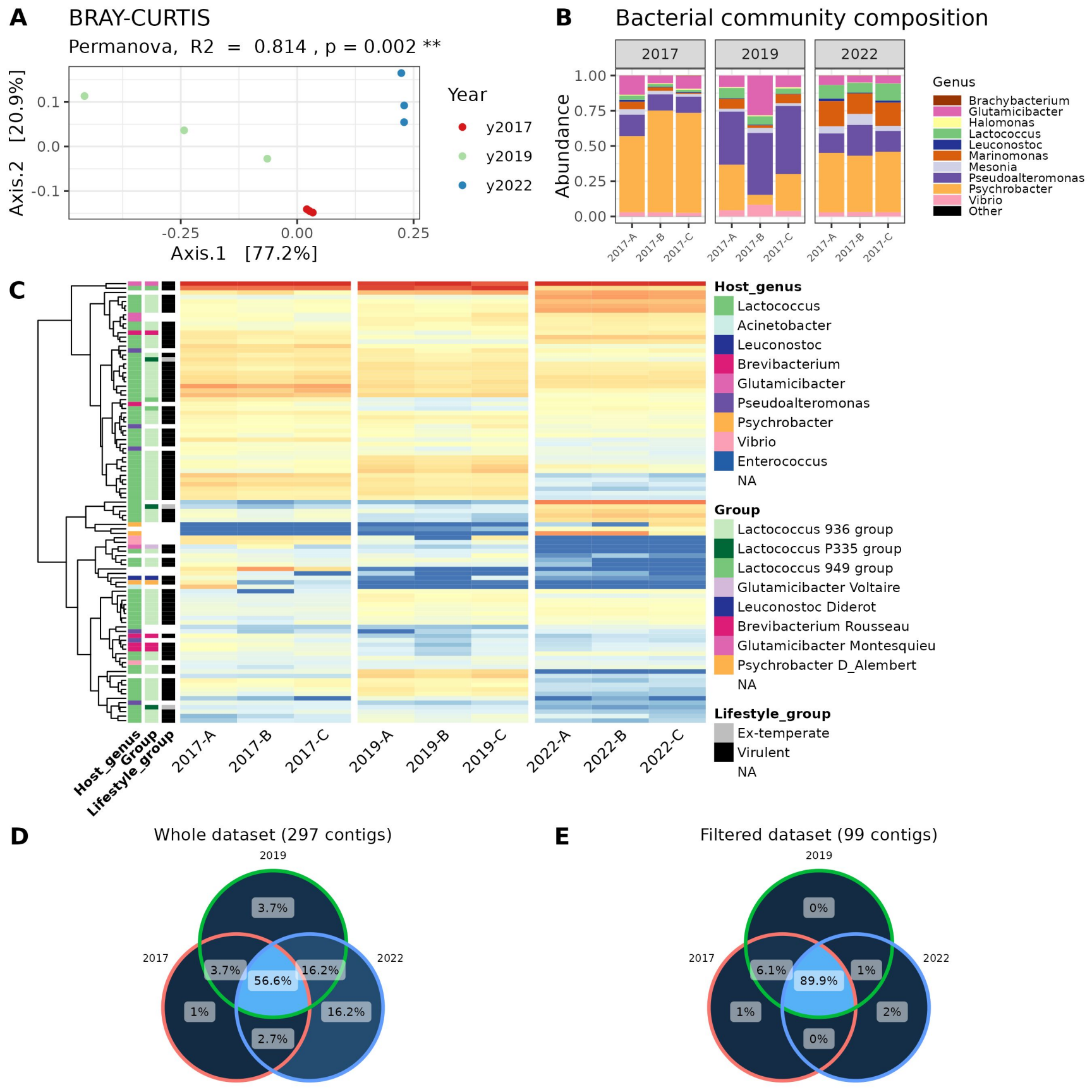
A
BRAY-CURTIS
Permanova, R2 = 0.814 , p = 0.002 **
Axis.2 [20.9%]
Axis.1 [77.2%]
Year
y2017
y2019
y2022
B
Bacterial community composition
2017
2019
2022
Abundance
Genus
Brachybacterium
Glutamicibacter
Halomonas
Lactococcus
Leuconostoc
Marinomonas
Mesonia
Pseudoalteromonas
Psychrobacter
Vibrio
Other
C
Host_genus
Lactococcus
Acinetobacter
Leuconostoc
Brevibacterium
Glutamicibacter
Pseudoalteromonas
Psychrobacter
Vibrio
Enterococcus
NA
Group
Lactococcus 936 group
Lactococcus P335 group
Lactococcus 949 group
Glutamicibacter Voltaire
Leuconostoc Diderot
Brevibacterium Rousseau
Glutamicibacter Montesquieu
Psychrobacter D_Alembert
NA
Lifestyle_group
Ex-temperate
Virulent
NA
Host_genus
Group
Lifestyle_group
2017-A
2017-B
2017-C
2019-A
2019-B
2019-C
2022-A
2022-B
2022-C
D
Whole dataset (297 contigs)
2019
2017
2022
3.7%
3.7%
56.6%
16.2%
1%
16.2%
2.7%
E
Filtered dataset (99 contigs)
2019
2017
2022
0%
6.1%
89.9%
1%
1%
2%
0%